

Moisture uptake of a nonwoven geotextile carrier-GCL from Lateritic subsoils under simulated tropical thermal conditions

Fernando Henrique Martins Portelinha^{1#} , José Wilson Batista da Silva¹ ,
Natalia de Souza Correia¹ 

Article

Keywords

Geosynthetic clay liner
GCL hydration
Barrier system
Temperature
Pollution of underlying soil

Abstract

Environmental conditions have become a concern when involving the use of Geosynthetics clay liners (GCLs) as leachate barriers, particularly because they can be subjected to daily thermal cycles during construction and operation of landfills, which can affect their properties. This paper investigates the hydration behavior of a nonwoven geotextile carrier-GCL in contact with lateritic subsoils under isothermal and simulated thermal conditions as commonly found in tropical regions. A thermal insulate testing box was used to shelter an instrumented liner landfill allowing the investigation of thermal and hydraulic responses during hydration. Lateritic subsoils were observed not to provide high levels of GCLs hydration under isothermal conditions, whereas thermal daily cycles led to capillary break that restricted the moisture uptake at the interface between subsoil and the nonwoven geotextile carrier. Higher values of subsoil initial moisture contents were found to be significant to reduce capillary effects and to allow some GCL hydration. The poor hydration demonstrated to be critical in terms of GCL hydraulic behavior.

1. Introduction

Landfill liner systems have been designed with innovative barrier materials to prevent the pollution of underlying soil and groundwater by effectively controlling leachate contamination. Geosynthetics clay liners (GCL) have been used as barriers for containment of risky pollutants such as mining, municipal and industrial wastes, as well as ponds storages and others. In a landfill liner system, GCLs are overlain by a geomembrane and are allowed to hydrate from the subsoil before contact with leachate (Yu & El-Zein, 2020). This pre-hydration has been reported to be crucial for the proper effectiveness of GCLs under operation (Rowe, 2020).

The bentonite present in GCLs must hydrate at moisture content values above 80% to effectively perform as a fluid barrier (Chevrier et al., 2012; Rowe, 2020). An adequate GCL hydration improves self-healing, cation exchange capacity, as well as reduces bentonite erosion and shrinkage. However, although GCLs are commonly assumed as fully hydrated by the underlying foundation soil, field and laboratory investigations have proven that several factors may compromise GCLs hydration under operational conditions (Rowe et al., 2011; Rowe, 2020; Silva et al., 2022).

The complex issues involving GCLs hydration from underlying subsoils under certain conditions have been the focus of several investigations. Studies evidenced different factors that can impact GCL hydration, such as bentonite characteristics (Rowe, 2020), the amount of fines and smectite in the subsoil, as well as soil compaction properties (Rayhani et al., 2011; Acikel et al., 2018; Azad et al., 2011; Bouazza et al., 2017; Bradshaw et al., 2013; Bradshaw & Benson, 2014; Chevrier et al., 2012; Meer & Benson, 2007; Rowe, 2020). Studies indicate that GCL hydration is highly dependent on the type of permeant liquid and the cations present in the subsoil porewater (Rowe et al., 2019; Rowe & Li, 2021). Also, the characteristics of the GCL were observed to affect hydration performance, such as bentonite grain size distribution and mass per unit area (Guyonnet et al., 2009; Beddoe et al., 2011; Liu et al., 2015; Rowe et al., 2019; Yesiller et al., 2019), bentonite mineralogy (Rouf et al., 2016), and bentonite pore structure and heterogeneity (Acikel et al., 2018). Another GCL characteristic that influences its hydration is the type of carrier geotextile in contact with the foundation soil (Rowe, 2020). Acikel et al. (2018) revealed that nonwoven geotextile carriers are more prone to provide capillary break than woven geotextiles in contact to some types of subsoil.

[#]Corresponding author. E-mail address: sportelinha@ufscar.br

¹Universidade Federal de São Carlos, Departamento de Engenharia Civil, São Carlos, SP, Brasil.

Submitted on September 22, 2022; Final Acceptance on December 18, 2023; Discussion open until May 31, 2024.

<https://doi.org/10.28927/SR.2024.009722>



This is an Open Access article distributed under the terms of the Creative Commons Attribution License, which permits unrestricted use, distribution, and reproduction in any medium, provided the original work is properly cited.

In addition, moisture uptake is limited to vapor phase of water at the first contact, delaying or even reducing the GCL hydration when the nonwoven carrier is in contact with the subsoil.

Daily thermal cycles are also reported as a significant affecting factor on GCLs behavior (Koerner & Koerner, 2005; Thiel & Richardson, 2005). Laboratory investigations have been conducted using temperature-imposed cycles to investigate the impact of thermal effects on GCLs pre-hydration from subsoils (Rowe et al., 2011, 2013; Anderson et al., 2012; Sarabian & Rayhani, 2013; Hoai & Mukunoki, 2020). Rowe et al. (2011) evaluated the hydration of sodium bentonite GCLs uptaken from subsoils under different conditions and subjected to simulated daily thermal cycles. Daily thermal cycles were found to control the GCL hydration leading to final moisture contents between 14 and 30% depending on the initial suction of soil. Anderson et al. (2012) revealed that, under thermal cycles, GCLs hydration from clayey subsoils occur at a slower rate than sand and silt subsoils, and adversely affect the final equilibrium moisture content of GCLs. Sarabian & Rayhani (2013) reported that different GCLs exhibit different hydration behaviors under thermal conditions.

GCLs have been applied in different regions around the world, and contributions involving thermal cycles impact on GCLs hydration under tropical environment are scarce in the literature (Silva et al., 2022). Tropical countries are not only distinct in terms of climate conditions, but also for the large presence of lateritic subsoils. Lateritic soils are widely distributed throughout the world, occurring more frequently in the tropics and subtropics of Africa, Australia, India, South-east Asia, and South America. Lateritic soils underwent leaching processes during formation process, resulting in clay fractions essentially composed by kaolinite, often mixed with quartz, and hydroxides and hydrated oxides of iron and aluminum. These hydroxides favor the formation of aggregates of finer soil particles, a characteristic that explains the heterogeneity of pores in lateritic soils and the bimodal behavior of soil water retention curves (Durner, 1994; Chamindu Deepagoda et al., 2012; Portelinha & Zornberg, 2017). In regards of the reported issues involved in the application of GCLs in tropical regions, this study compares the hydration behavior of a nonwoven geotextile carrier-GCL in contact with lateritic subsoils under isothermal and simulated tropical daily thermal conditions. The effect of different initial moisture contents of lateritic subsoils on GCL hydration is also investigated. The effect of daily thermal cycles on the moisture uptake behavior of the GCL in contact with subsoils is discussed based on suction changes which provides the understanding of hydration process and the role of capillary effects. Post-hydration tests were also conducted in GCLs samples to investigate the effect of hydration process on the hydraulic conductivity, swell index, and cation exchange capacity.

2. Experimental program

2.1 Geosynthetic clay liner

The GCL used in this research is composed of a granular sodium-bentonite core, a needle-punched nonwoven carrier geotextile and woven geotextile cover. Properties of the GCL are summarized in Table 1. Free hydration tests were conducted to estimate the GCL reference water content (w_{ref}) using the water rising process under 1 kPa of confining stress (Acikel et al., 2018; Anderson et al., 2012; Rayhani et al., 2011; Sarabian & Rayhani, 2013).

The water retention curve (WRC) of a GCL is crucial information for the understanding of moisture uptake from subsoils. In this study, the WRC was obtained using the filter paper technique described by Barroso et al. (2006). According to Barroso et al. (2006), as GCLs present a low thickness, its total suction can be assumed as equal to the matric suction. The experimental values of the WRC of the GCL were obtained using wetting and drying processes. Figure 1a presents experimental data and fitting models used to define the WRCs of the GCL. The fitting parameters can be found in Silva et al. (2022). Water entry values (WEV) and air entry values (AEV) of the GCL are also indicated in Figure 1.

2.2 Subsoils

Two lateritic soils collected in the Sao Paulo State, Brazil, were used in this experiment. These soils were selected as typical lateritic soils commonly found in tropical regions around the world. The geotechnical properties of the lateritic soils are summarized in Table 2.

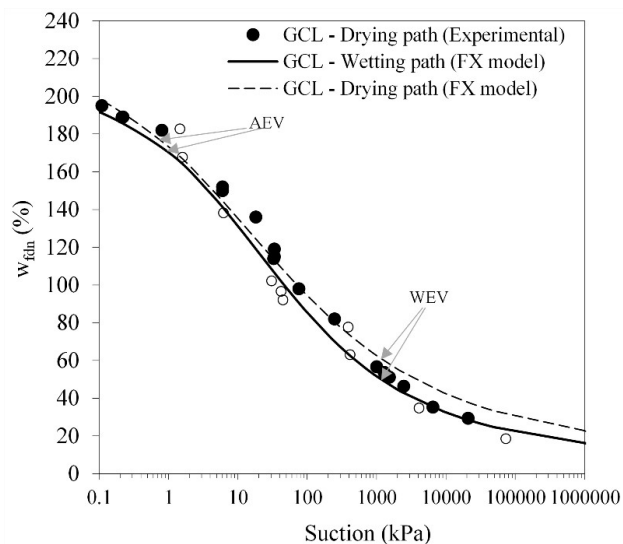


Figure 1. Water retention of the GCL.

According to the Unified Soil Classification System (USCS) (ASTM, 2017a), the first soil is considered a clayey sand (SC), and the second soil is classified as a high plasticity clay (CH). While the lateritic CH soil contains clay particles, it also has a significant percentage of fine sand (36%), which is common in lateritic soils. X-Ray diffractograms were used to investigate the minerals contained in the lateritic soils.

The quantification of the mineral phases was performed by the Reference Intensity Ratio (RIR) method (Dish, 2015). Table 3 presents the mineral contents in the lateritic soils and the notable presence of Hematite (Fe_2O_3), which characterizes the subgrade soils as ferruginous materials. The cation exchange capacity shown in Table 3 was obtained based on the ASTM D7503 (ASTM, 2018c).

Table 1. GCL properties.

		Properties	GCL
Bentonite	Particle type		Granular
	Aggregate size distribution (mm) (ASTM, 2017b)		
		D_{10}	-
		D_{30}	-
		D_{60}	-
		D_{90}	0.3
	Plastic Index (%) (ASTM, 2017c)		252
	Avg. Dry mass /area (g/m^2) (ASTM, 2018b)		4964
	Swell Index ($\text{ml}/2\text{g}$) (ASTM, 2019b)		25
	Fluid Loss (ASTM, 2019c)		18
Smectite content (%)		80	
Cation Exchange capacity ($\text{meq}/100\text{g}$) (ASTM, 2018c)		140	
Cover	Type		WGT
	Avg. mass /area (g/m^2) (ASTM, 2018a)		130
Carrier	Polymer		PP
	Type		NWGT
GCL	Avg. mass /area (g/m^2) (ASTM, 2018a)		200
	Polymer		PP
	Thermally treated		yes
	Bonding strength (ASTM, 2020b)		NP
	Thickness (mm) (ASTM, 2020c)		7.0
	Initial gravimetric water contents		21
	Reference gravimetric water content (%) (ASTM, 2019a)		182.7
Tensile strength (kN/m) (ASTM, 2020d)		12.0	
Peel strength (N/m) (ASTM, 2020e)		150	
Hydraulic conductivity (m/s) (ASTM, 2020a)		1.2×10^{-11}	

Table 2. Properties of lateritic soils.

Properties	SC	CH
Sand content (%) (ASTM, 2007)	67.5	36.0
Silt content (%)	5	9
Clay content (%)	27.5	55.0
Specific gravity (ASTM, 2014)	2.80	2.98
Liquid limit, LL (%) (ASTM, 2017c)	33	51
Plastic limit, PL (%)	22	27
Plastic Index, PI (%)	11	24
Maximum dry density (g/cm^3) (ASTM, 2012)	1.77	1.68
Optimum moisture content (OMC) (%)	14.8	24.0
Cation exchange capacity ($\text{meq}/100\text{g}$) (ASTM, 2018c)	3.28	8.44
Hydraulic conductivity at OMC (m/s) ^a	5.6×10^{-6}	3.4×10^{-7}
Hydraulic conductivity at OMC+2% (m/s) ^b	4.2×10^{-7}	1.6×10^{-8}

^aCompacted at OMC and 95% degree of compaction; ^bCompacted at OMC+2% and 95% degree of compaction.

Table 3. Mineral contents of lateritic soils.

Subsoil	Quartz	Kaolinite	Gibbsite	Goethite	Hematite	Other
SC	50%	6.2%	7.2%	0.2%	15.3%	21.1%
CH	17.2%	23.2%	11%	8.8%	25.2%	14.6%

In order to evaluate the unsaturated hydraulic properties of the compacted soils, the filter paper technique (ASTM, 2016) was used to obtain the water retention curve (WRC) by drying and wetting processes. Samples were prepared at 95% of the dry unit density of Standard Proctor compaction tests. Figure 2 shows the WRCs of the lateritic soils, including fitting models, air and water entry values (AEV and WEV, respectively). The SC soil curve (Figure 2a) was fitted using a bimodal model by Durner (1994), while the CH soil curve (Figure 2b) was fitted by the equation of Fredlund and Xing (Fredlund & Xing, 1994).

In Figure 2b, CH soil presents WRC of unimodal behavior, which is coherent with the homogeneous granulometric distribution of this soil. The bimodal behavior shown in the WRC of SC soil (Figure 2a) is the result of macro and micro pores in the soil structure. In these cases, the macro pores of the soil are formed by the soil granular structure, composed of sand and fine aggregates (clay and silt). Micro pores are present in aggregations of clay minerals commonly found in lateritic soils (clay and silt), given by the presence of iron and aluminum oxides (Maignien, 1966).

2.3 GCL hydration test under isothermal condition

The configuration of GCL hydration tests in isothermal condition adopted in this study is shown in Figure 3. Polyvinyl chloride (PVC) cells of 250 mm in diameter and 500 mm in height were constructed to investigate the closed-system (i.e., constant mass of moisture) hydration of three GCLs installed over lateritic subsoils. Both soils were mixed with distilled water to bring moisture contents to compaction values. For each subsoil, compaction moisture contents adopted were at optimum (OMC) and 2% above optimum (OMC + 2%). Different moisture content conditions of the subsoil were evaluated in the search of a better GCL hydration. Each hydration cell was compacted in 10 layers of 40 mm height soil targeting 95% of degree of compaction in relation to the Standard Proctor effort. Once the compaction process was complete, the hydration cells were sealed with a cap to assure moisture equilibrium. A moisture content sensor similar to those used in thermal tests was installed in the subsoil at 20 mm below the GCL to capture moisture changes during hydration process.

GCL samples were extracted from the roll, cut in 250 mm diameter, and placed over the subsoil (after moisture equilibrium) with as-received GCL moisture content (Table 1), as conducted in thermal tests. The GCL sample was installed with the nonwoven geotextile face in contact with the subsoil. After the GCL installation, it was covered by a geomembrane (GM) to minimize potential evaporation of moisture into the space above the GCL, simulating a landfill cell condition. A surcharge of 1 kPa composed of gravel layer was placed over the GM to improve the contact between The GCL and subgrade soil.

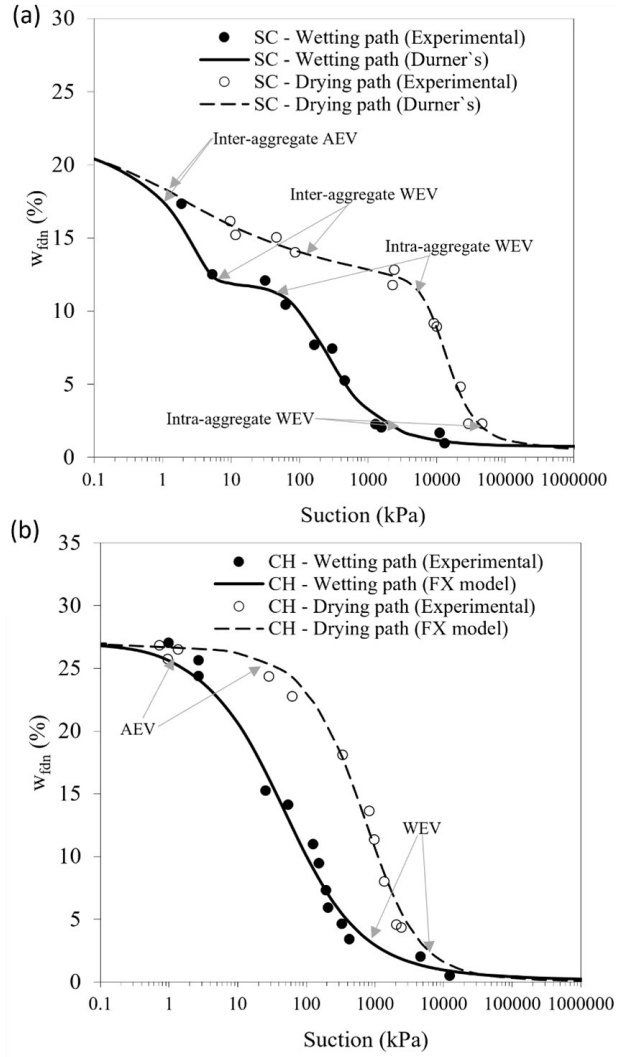


Figure 2. Water retention of the subgrades: (a) SC soil; (b) CH soil.

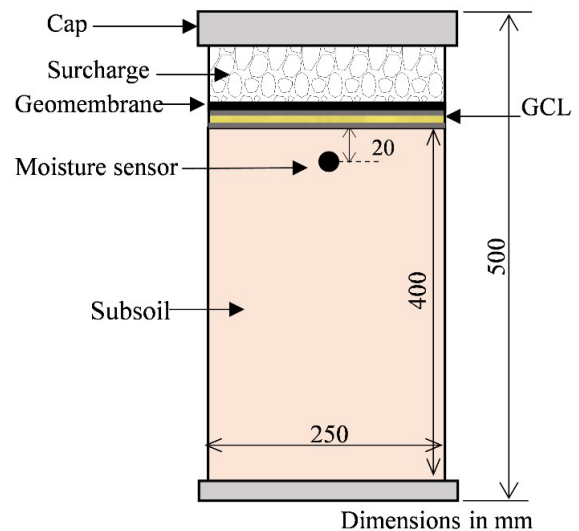


Figure 3. Isothermal hydration testing setup.

The same surcharge level was used by Rayhani et al. (2011), Anderson et al. (2012), Sarabian & Rayhani (2013) and Acikel et al. (2018). Then, the system was sealed. Tests were conducted under environment-controlled conditions of 21 °C.

GCL gravimetric moisture contents were monitored weekly to evaluate the progression of GCL hydration from the lateritic subsoils using a digital scale of 0.01 g precision. The GCL water content was obtained by weighing the samples in a less than 5 minutes process to return GCLs to the PVC cell without significant loss of moisture. At the end of each test, soil samples were extracted along the column height (40, 80, 120, 160, 200, 240, 280, 320, 360 and 400 mm) to measure soil gravimetric moisture contents. After tests, GCL samples were weighted, bagged, and stored in an insulated and hermetic box at room temperature to conduct post-hydration tests, such as swell index, cation exchange capacity and hydraulic conductivity tests.

2.4 Thermal-cycling hydration tests

To investigate the GCL hydration from lateritic subgrades exposed to thermal cycles, a physical model was constructed allowing the evaluation of the liner materials under simulated heating/cooling cycles. Figure 4 illustrates the geometry and instrumentation used in the thermal cycling tests. Moisture sensors EC-5 (EM50) and thermocouples (-55 to 125 °C ± 0.25 °C) were embedded at different depths of the subsoil to capture moisture content and temperature profiles. The type of sensor adopted in this investigation measures volumetric water content via dielectric constant of the soil using capacitance technology with frequency of 70 MHz. The test box was built with plasticized wood, with internal dimensions of 650 × 360 × 600 mm, faces coated with a 60 mm thick Styrofoam isolation layer with objective of avoiding heat exchanges. The same compaction process adopted in the isothermal hydration tests was performed in the thermal cycling hydration tests.

The GCL was cut into 650 mm long and 360 mm wide specimens to fit the internal box dimensions. After being carefully cut, specimen edges were sealed using wetted bentonite to avoid bentonite loss. The GCL specimens were then installed over the compacted lateritic subgrade at as-received initial moisture content with the nonwoven geotextile side in contact with the subsoil. The same type of geomembrane used in the isothermal tests was placed over the GCL in the thermal-cycling hydration tests. Both GM and GCL were restrained longitudinally by bar clamps to reproduce the anchorage of GCL panels. Similar anchoring models have been used in other laboratory studies (Koerner & Koerner, 2005; Thiel et al., 2006; Rowe et al., 2013). A surcharge layer (gravel layer) of 1 kPa was placed over the anchorage panel to improve contact between the GCL and subsoil. To simulate daily heating/ cooling cycles, a heating mattress was installed over the surcharge layer. The daily cycle of temperature adopted in this study is shown

in Figure 5, which was chosen based on internal temperatures reported in Brazilian landfills (Costa et al., 2019; Silva et al., 2020; Portelinha et al., 2020). A heating period of 8 hours was imposed with a temperature of 57 ± 4 °C, followed by a cooling period of 16 hours, leading to a minimum of 30 ± 4 °C of temperature in a day cycle.

Thermal cycling hydration tests were performed using the GCL in contact with the CH subsoil at OMC the period of 31 days. Thermal cycling hydration tests conducted on OMC + 2% run for longer periods, 63 days for CH subsoil and 56 days for SC subsoil. The GCL shrinkage was also periodically monitored by measuring GCL dimensions changes during tests. Figure 6 depicts a typical internal temperature response measured inside the subsoil over time in cycling hydration tests at 40 mm and (Figure 6a) and at 80, 120, 160 and 240 mm of depth (Figure 6b).

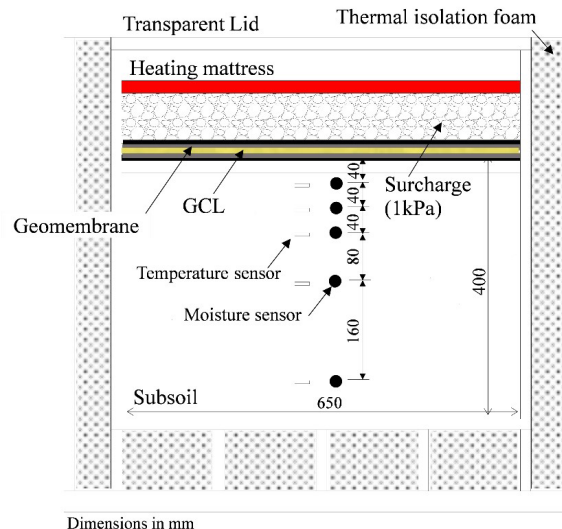


Figure 4. Schematic of the test box for thermal cycling tests.

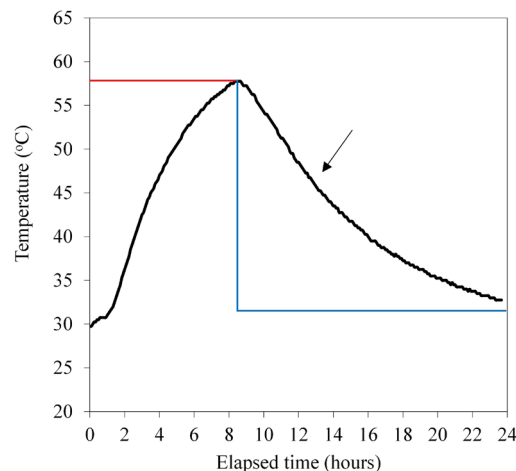


Figure 5. Daily thermal cycle.

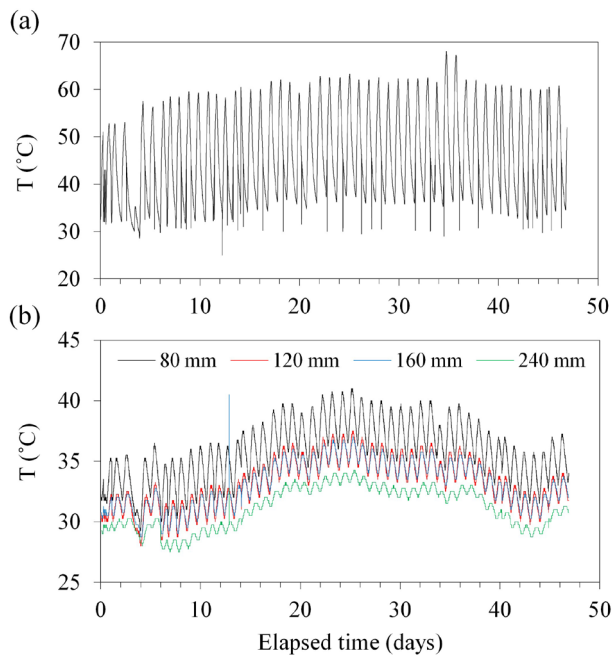


Figure 6. Temperatures registered inside the subsoil CH at OMC over time: (a) at 40 mm of depth; (b) at 80, 120, 160 and 240 mm of depth.

2.5 Post-hydration permeability tests

Post-hydration tests were conducted to investigate how insufficient hydration affected GCL hydraulic conductivity exposed to isothermal and thermal conditions. Hydraulic tests were conducted with deionized water according to ASTM D5887 (ASTM, 2020a). The flow index test was conducted using a flexible wall permeameter as described in ASTM D5887 (ASTM, 2020a). The GCL was saturated by backpressure and subsequently permeated under high levels of hydraulic load. The flux was imposed from the base to the top of the sample. The GCL sample was placed between two porous stones in a test cell with a confining pressure of 400 kPa and a backpressure of 365 kPa until saturation. Once saturated, an inflow of water with a pressure of 525 kPa and an outflow with a pressure of 515 kPa was imposed, and the inflow and outflow water were measured over time. The calculation of the flow value was determined within an interval of 8 hours when the ratio between water inflow and outflow attended the range of 0.75 and 1.25 at three consecutive intervals. The hydraulic conductivity was then obtained assuming the GCL thickness after test.

3. Results and discussions

3.1 Thermal behavior of the subsoils against daily cycles

The responses of temperature sensors installed at different depths of the subsoil are shown in Figure 7 as a typical thermal

response observed in all tests. Mostly, the thermal cycles led to higher temperatures and more variation at points close to the GCL layer and lower temperatures as deeper the measurement points. The daily variation of temperature is also shown to reduce with soil depth. Note that temperatures varied from 30 °C to 50 °C at 40 mm of depth (Figure 7a), which approximates to the applied daily temperatures imposed in the thermal daily cycles. At 80 mm of depth (Figure 7b), the temperature was significantly lower, ranging from 30 to 40 °C. At the deepest measuring point, daily temperature variation was found to be around 2 °C. Although the applied thermal daily cycle was the same over time, temperatures seem to accumulate over time for all measuring points at 80 mm or deeper. This behavior was observed in all thermal tests conducted in the experimental program.

Temperatures measured inside the subsoil allowed defining profiles at different times along daily thermal cycle tests. Figure 7a shows temperature profiles at the beginning and at the peak of the 20th cycle, for all test conditions (CH-OMC, CH-OMC + 2% and SC-OMC + 2%). It should be noted that, in all the tests, temperature was uniform along the depth at the beginning of the cycle with values ranging from 35 to 37 °C. When the peak daily temperature is reached, the first 40 mm was slowly raised to 40 to 65 °C (Figure 7b), while temperatures were found to be uniform along higher depths. Despite the difference in foundation type and moisture contents, the temperature in SC subsoil at OMC + 2% were generally higher than the CH at OMC + 2%, while the CH subsoil at OMC had lower levels of temperature among all tested. This is because the heat transfer is expected to be higher for the soil at higher moisture content. Similar results were observed by Rowe et al. (2011). The reason for higher temperatures in the SC soil was not fully understood in this study and demands additional research. A potential motivation would be the micro aggregations in this type of soil.

3.2 Effect of daily thermal cycles on GCL hydration

Figure 8 compares the hydration of GCL from the lateritic SC subsoil at OMC + 2% under isothermal and thermal conditions. Changes in the subsoil moisture content (w_{fdm}) over time measured at the depth of 40 mm are also shown in Figure 8. The influence of thermal conditions was observed to have a considerable effect on the GCL hydration, as also observed by Rowe et al. (2011), Anderson et al. (2012) and Sarabian & Rayhani (2013). Under tropical thermal condition, the lateritic SC subsoil at OMC + 2%, was not able to hydrate the GCL even after 56 days (8 weeks) of contact. At same time, the moisture content of the subgrade reduced over time until a certain limit, which indicates the disequilibrium caused by the suction gradient between GCL and soil. The reduction in SC subsoil moisture content over time without increases in GCL hydration indicates a restriction of upward flow at the interface between the subsoil and GCL, which is typical of capillary barrier effects.

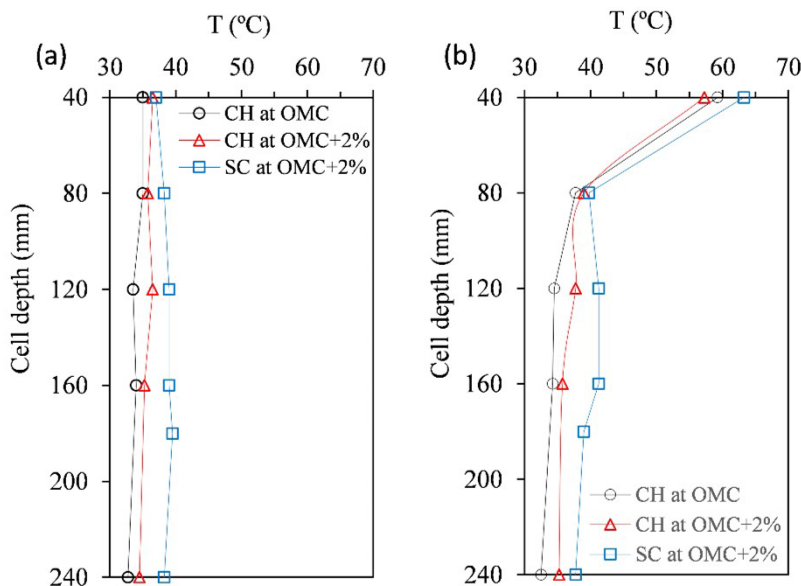


Figure 7. Temperatures measured along the depth of the subsoil: (a) at the beginning of the 20° cycle; (b) at the end of the 20° cycle.

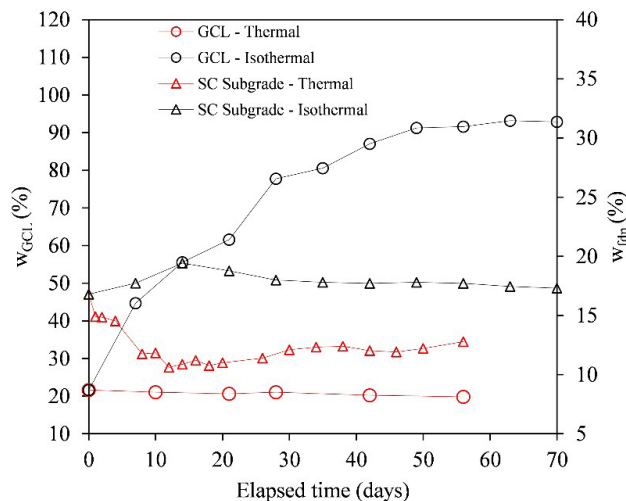


Figure 8. Comparison of GCL hydration from SC subsoil at OMC + 2% under isothermal and thermal conditions and SC soil moisture data in thermal tests.

This is a potential consequence of installing the nonwoven face of geotextile in contact with the subsoil (Silva et al., 2022). After 20 days the moisture content of the subgrade turns to rise indicating water precipitation from the GCL or water accumulation due to capillary break effects. Basically, the water available to redistribute is from the inter aggregates voids and the relatively low amount of water in the voids did not hydrate the GCL enough to reduce suction and to allow the breakthrough of water. The same did not occur under isothermal conditions. The moisture uptake is clearly observed as both subsoil and GCL moisture contents varied over time. There is an increase in GCL hydration over the

time, but in levels relatively lower than those suggested as sufficient for a proper performance in field (Hosney et al., 2016; Rowe et al., 2019; Rowe, 2020). It is also interesting to note the increase in the SC subsoil moisture content because of an upward flow led by the changes in suction gradient between GCL and subsoil, which affects the hydration equilibrium. Under isothermal condition, the subgrade moisture content practically did not change during GCL hydration.

Similar effects were observed in the GCL in contact with the CH at OMC (Figure 8a). Figure 9 compares the hydration of GCL from CH lateritic subsoil at OMC and OMC + 2% under isothermal and thermal conditions, as well as changes on subsoil moisture contents at 40 mm of depth during the tests. Like the lateritic SC soil (Figure 8), the influence of thermal conditions was significant to restrict GCL moisture uptake from the CH soil at OMC in comparison to the isothermal conditions (Figure 9a). As observed in isothermal tests, the higher the soil initial moisture content, higher was the GCL hydration under tropical thermal conditions, although the hydration levels were very low. Suction levels provided by the relatively low initial moisture content led to capillary break effects at the subsoil-GCL interface which affected the GCL hydration (Figure 8a) from the drier subsoil. This effect is reduced in tests conducted with the CH subsoil at OMC + 2% (Figure 9b) due to the higher initial moisture content and consequent lower suction. Note in Figure 9b that the moisture content of the subsoil reduced in the first 5 days, whereas the GCL is not hydrated. This fact indicates capillary effect temporarily acting at the interface. After 5 days, the moisture content turned to increase and the GCL moisture uptake started, indicating the capillary breakthrough and the establishment of the upward flow due to suction gradient between GCL and subsoil.

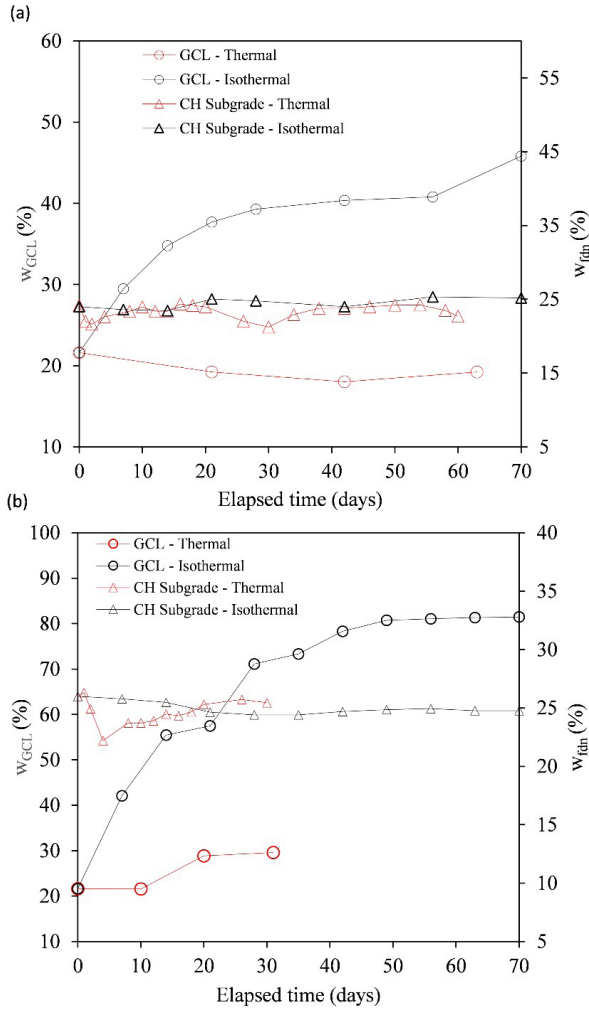


Figure 9. Comparison of GCL hydration from under isothermal and thermal conditions and soil moisture data in thermal tests: (a) CH at OMC; (b) CH at OMC + 2%.

Figure 10 shows the moisture content profiles of the subsoil after different thermal cycles for tests using the SC at OMC + 2%, CH at OMC and CH at OMC + 2% (Figures 10a, 10b and 10c, respectively). Data shows an overall trend of moisture content reductions because of cumulative daily cycles until 20th cycle, excepting in the case of CH at OMC subgrade. After that, moisture contents oscillated because of hydration disequilibrium over time. It is expected to have reductions in moisture content only at approximately 100 mm of depth since temperatures varied more significantly in this upper portion of the subsoil. The reduction in soil moisture contents in upper layers also affected deeper soil portions evidencing an upward flow effect. Note in Figure 10c, in which a wetted soil was used, the upward flow was limited to the first 150 mm for the period of test adopted herein. Note that the capillary break effect observed for the SC at OMC + 2% and CH at OMC (Figures 9a and 9b) promotes a disequilibrium on upward flow changing the moisture profiles over the applied cycles. It is also believed that the volume of water that flows up is concentrated at the proximity of the GCL, in which capillary break occurred, and not captured due to the lack of sensors at the proximity. As temperatures change during the daily cycle, the water tends to move constantly, whose are not sensitive enough to be captured by moisture content sensors.

3.3 Suction analyses of GCLs and lateritic subsoils under isothermal and thermal conditions

A clear understanding of water distribution between GCLs and subsoils during hydration is obtained when comparing suction data and WRCs of both materials. According to Acikel et al. (2018), GCLs have a tri-modal pore structure defined by geotextile pores (macro-pore), inter-aggregate bentonite pores (meso-pores) and intra-aggregate pores,

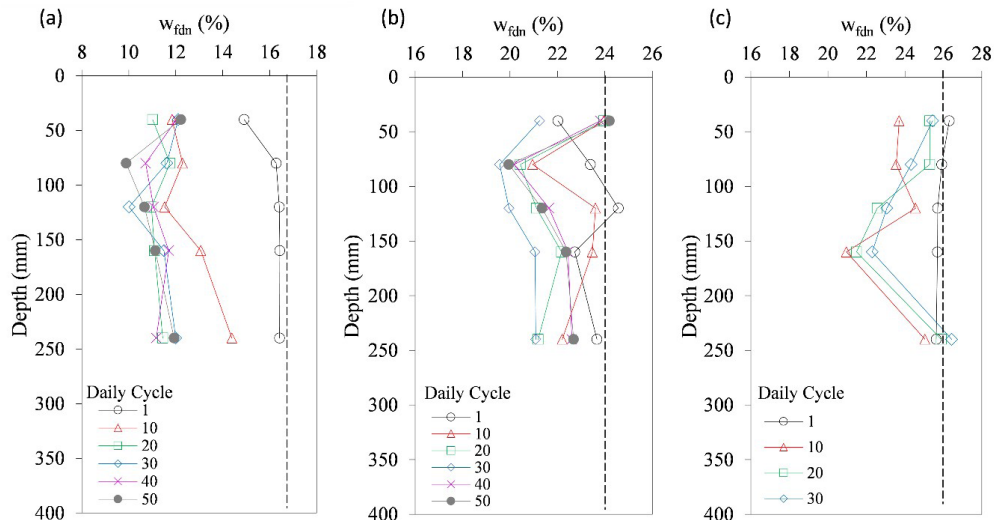


Figure 10. Effect of thermal cycles on water content profile of subsoils: (a) SC at OMC; (b) CH at OMC; (c) CH at OMC+2%.

and any bentonite pores smaller than intra-aggregate as micro-pores. An overlapping within these pore ranges can possibly occur leading the GCLs components (bentonite and geotextiles) to experience different wetting behavior. This tri-modal pore distribution affects water redistribution from the soil to the GCL and can lead to capillary breaks. The difficulty of a GCL to hydrate from a subsoil can be understood following the WEVs in the WRC of the GCLs (wetting path) and AEVs in the WRC of the subsoil (drying path). Critical hydration behavior of GCLs is, in the case of the suction values, higher than that corresponding to the WEV, a situation in which capillary connections are not formed, and capillary break is expected to develop. When the suction range is higher than the WEV of the GCL, but lower than the residual suction limit of the subsoil, water redistribution is also affected and GCL acceptable hydration levels are not reached. When the GCL has suction ranges lower than the WEV and the residual suction of soil, GCL hydration is expected to reach higher levels.

Figures 11 shows the GCL and subsoils suction analyses in isothermal and thermal hydration tests for lateritic SC and CH soils at OMC + 2%, respectively. Soil suction values were obtained using moisture sensors data and their corresponding values of suction in each WRC. It is worth mentioning that the contact filter paper test measures matric suction up to a limit and, if exceeded, it measures total suction due to the permeable membrane effect (Marinho & Gomes, 2012; Acikel et al., 2018). Figures 11a and 11b compare suction data of GCLs over time, while Figures 10c and 10d compare subsoils suction over time. The suction behavior of the GCL under isothermal conditions was practically the same for both subsoils with slightly lower values for the CH materials because of its greater moisture content. Note that in both cases, the suction values became lower than the GCL WEV which indicates capillary connections developing and hydration occurring. Note that better hydration occurred when the subgrade suction value was close or lower than the AEV.

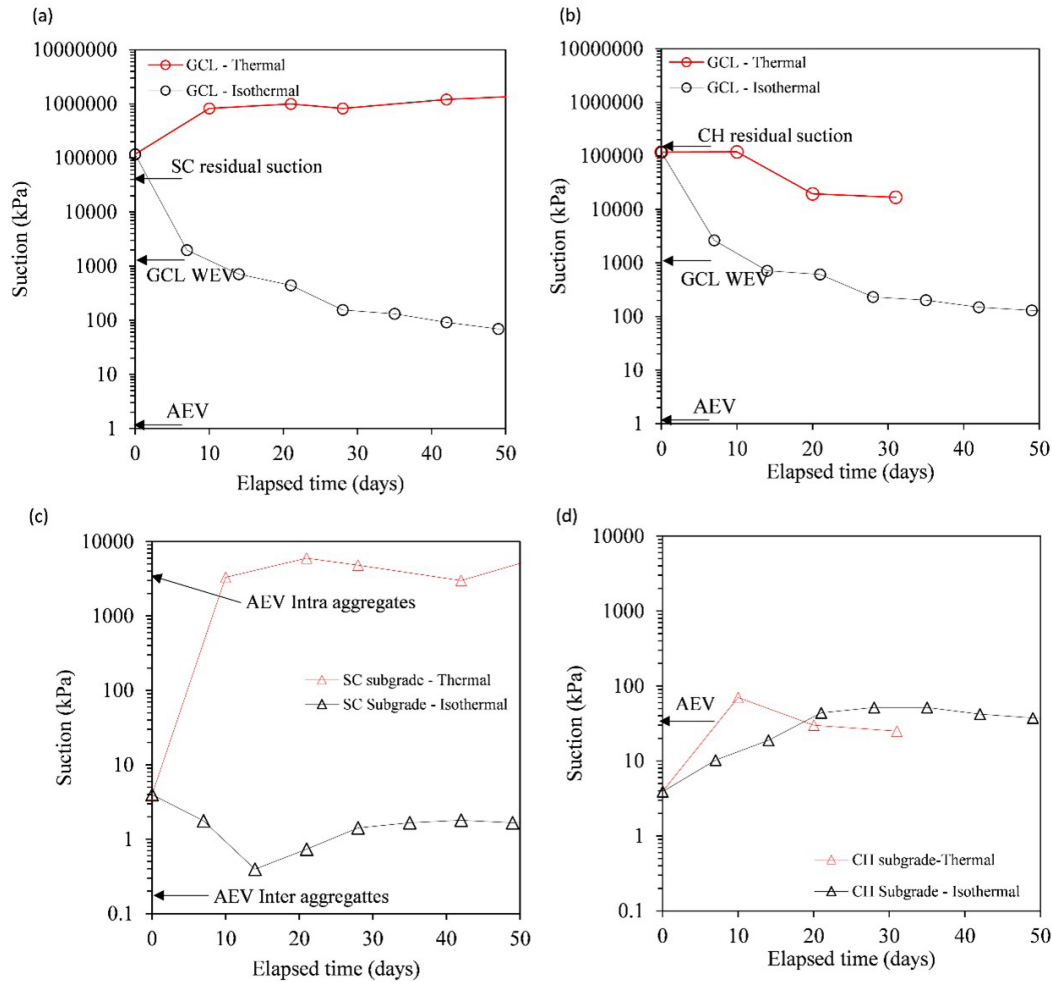


Figure 11. Suction analyses between GCL and subsoil during isothermal and thermal hydration tests: (a) GCL suction progress with SC subsoil at OMC + 2%; (b) GCL suction progress with CH subsoil at OMC + 2%; (c) SC subsoil at OMC + 2% subsoil suction; (d) CH subsoil at OMC + 2% subsoil suction.

In contrast, thermal conditions led to the increase in GCL suction in contact with the SC subsoil keeping it with values greater than the WEV. This means that capillary breaks affected the hydration from the SC subsoil during the test under daily thermal condition. It should be noted that capillary effect also happened with the CH subsoil, but with a different reduction in suction (from 100000 to 40000 kPa). This is evidence that some exchange of water happened but not sufficiently to promote the breakthrough of water. When suction values of the GCL were significantly higher than the WEV, capillary connection is harder to be achieved, which restrict the GCLs hydration, as reported by Acikel et al. (2018). Capillary break developed at the unsaturated interface is potentially restricting the upward flow and the GCLs hydration. The timid hydration of the GCL in contact with the CH at OMC + 2% is favored by GCL suction levels lower than the residual suction of the soil, allowing some capillary connections. However, hydration levels were still lower than the indicated as sufficient for a proper barrier performance (Rowe, 2020).

The progression of suction values of the subsoils at the depth of 40 mm for isothermal and thermal tests are presented in Figures 10c and 10d, respectively. The water redistribution between the GCL and subsoil is found not to reach an equilibrium. For the test using the SC subsoil at OMC + 2% (Figure 11c) under isothermal condition, suction reduced and then turned to increase to initial value. In the case of the CH subsoils, the suction increases and, at the 40th day, demonstrated a trend of decrease. The changes on suction gradient between soil and GCL led to constant changes in water upward flow and, as consequence, on the GCL hydration rate over time. In the case of thermal tests, subsoil suction increased with the GCL suction at the point located 40 mm deep from the GCL layer, for both subsoils. It is believed that capillary effects are concentrated water above the depth of 40 mm, which was not able to be captured by sensors. The GCL hydration in tropical thermal conditions simulated herein in a difficult task due to the high temperatures occurring over relatively long term and the dehydration is expected to occur. The investigation of initial suction values of the subgrade and the GCL have been found to be extremely important for an appropriate performance of GCL in liners systems.

3.4 Effect of hydration on the GCL properties

Figure 12 compares the results of swell index (SI), cation exchange capacity (CEC) and hydraulic conductivity (k) obtained after isothermal (I) and thermal (T) hydration tests conducted on the GCL. According to GRI GCL3 (Geosynthetic Institute, 2016), the minimum swelling index required for a bentonite used in a GCL is 24 mL/2g. Results in Figure 12a show that virgin samples of GCL reached the minimum required SI value. However, after hydration tests, in both thermal and isothermal conditions, all results

of SI reduced to lower levels than the minimum required to keep GCL swelling properties. In addition, SI values from tests conducted on post-test samples were lower than those of virgin (non-hydrated) tests. Results also show that SI of samples from isothermal tests were lower than of those from thermal tests, which is potentially related to the cation exchange during hydration process. Note that it occurred only for tests in which some water distributions happened, such as the test with CH at OMC + 2% subsoil. In Figure 12c, CEC values presented a similar trend of SI after tests.

Figure 12b compares results of saturated hydraulic conductivity of virgin GCL samples with results of saturated hydraulic conductivity of exhumed GCL samples after hydration tests. As reference, the GRI-GCL3 suggests the maximum value of hydraulic conductivity as 5×10^{-11} m/s.

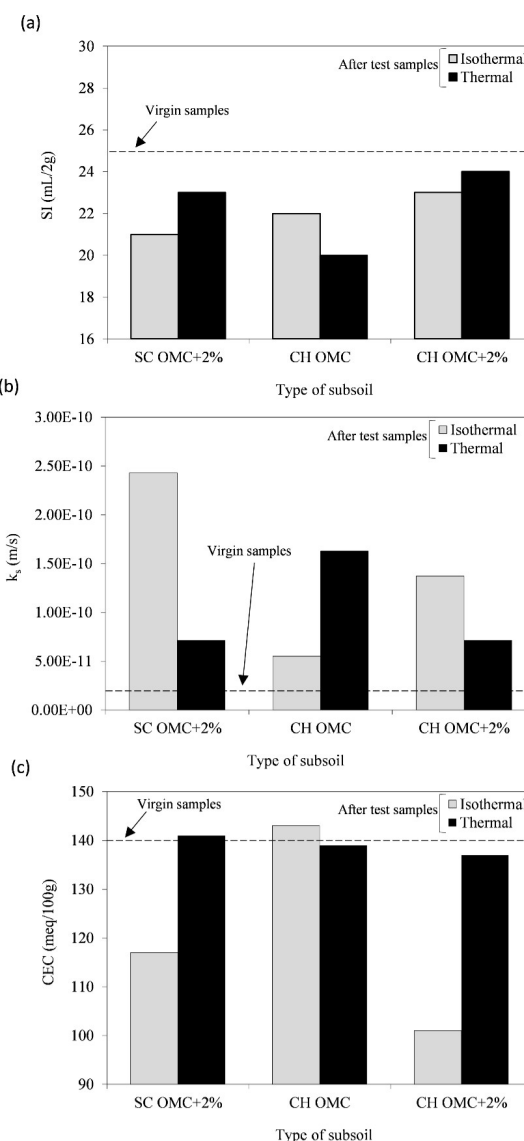


Figure 12. GCL properties after hydration tests: (a) SI ; (b) hydraulic conductivity; (c) CEC .

Note that the GCL is impacted in a such degree by some hydration scenarios that it alters the hydraulic conductivity to values higher than that suggested by the GRI. In general, an increase in the saturated hydraulic conductivity of the GCL was observed in both soils at isothermal conditions after hydration tests. Values of hydraulic conductivity were observed to be higher in samples from isothermal than from thermal hydration tests, potentially due to cations exchanges between the subsoil and the GCL. In the case of the GCL hydrated from the CH soil at OMC, samples from thermal tests had higher hydraulic conductivity than those from isothermal. In this case, internal cracking would have a more pronounced effect.

According to Acikel et al. (2018), cation distribution due to self-diffusion in bentonites is favored by wetting, which leads to more significant changes in GCL behavior. In thermal-cycles tests, as no moisture increase was seen in subsoils and GCLs due to the capillary break, less cations exchanges could happen, and consequently alterations in hydraulic conductivity are essentially due to the loss of moisture as a thermal effect. Results in Figure 12c confirm no significant alterations in *CEC* values after thermal cycle tests. On the other hand, analysis conducted under isothermal conditions presented alterations in bentonite *CEC* after tests, mainly for soils compacted at OMC + 2%. Thermal test specimens did not reach the hydration level to have these impacts. Nonetheless, all GCLs presented *CEC* values greater than the minimum 70 meq/100g (Guyonnet et al., 2009) even after GCL hydration tests.

4. Conclusions

This paper evaluates the effect of typical tropical daily thermal cycles on the hydration behavior of a GCL in contact with two different lateritic subsoils. Based on this experimental program, the following conclusion can be drawn:

- The effect of tropical daily thermal cycles over the liner system reflected in significant increases in soil temperature at the first 80 mm of depth. Temperatures inside the soil seem to accumulate and occasionally oscillate over time mainly in points deeper than 40 mm, but at smaller levels than upper points. In addition, temperatures were greater as higher soil degree of saturation;
- The GCL in contact with the tropical subsoils was found not to sufficiently hydrate under isothermal conditions. Under tropical daily thermal conditions, the GCL presented no hydration. High temperatures led to high suction levels of GCLs, which favored capillary break effects. This effect was found to be reduced as higher the initial moisture contents of the subsoil;
- Under thermal conditions, lateritic clayey soils (named CH in this investigation) promoted equal or better conditions to hydrate the GCL than the SC sandy soils. The opposite behavior was observed under isothermal conditions;

- Although temperatures were greater at upper portions of the subsoil, the reduction in soil moisture contents in deeper soil portions evidenced an upward flow effect. Changes in the internal temperature led to constant changes in subsoil moisture content profiles;
- Suction analyses demonstrated that greater hydration was reached with greater initial suction gradients and when soil suction is close to or lower than soil AEV. The relatively lower initial gradient of the CH soil led to a certain difficulty of the GCLs to hydrate as compared to SC soil under isothermal condition. When the initial suction values of the GCLs are higher than its WEV, capillary break occurs in the beginning of the hydration. The temperature elevated suction values and favored the capillary effect;
- The swell index, *CEC* and hydraulic conductivity of the GCL samples exhumed from tests were altered when compared to virgin samples. GCLs properties were more affected by hydration in isothermal condition due to cation exchange provided by the large amount of water involved in the water redistribution.

Acknowledgements

This study was financed in part by the Coordenação de Aperfeiçoamento de Pessoal de Nível Superior - Brasil (CAPES) - Finance Code 001. Authors are grateful to the technical staff of the Laboratory of Geotechnics and Geosynthetics of the Federal University of Sao Carlos. Authors thank Huesker, Ober and CETCO for providing the geosynthetics.

Declaration of interest

The authors have no conflicts of interest to declare. All co-authors have observed and affirmed the contents of the paper and there is no financial interest to report.

Authors' contributions

Fernando Henrique Martins Portelina: Supervision, Conceptualization, Data curation, Visualization, Writing – original draft. José Wilson Batista da Silva: Conceptualization, Tests execution, Formal Analysis. Natalia de Souza Correia: Supervision, Conceptualization, Analysis review, Visualization, Writing – review & editing.

Data availability

The datasets generated analyzed during the current study are available from the corresponding author upon request.

List of symbols

k	Hydraulic conductivity
w_{fdn}	Subgrade (or foundation soil) moisture content
w_{ref}	Reference moisture content
AEV	Air entry value
ASTM	American Standard Association
CEC	Cation exchange capacity
CH	High plasticity clay
GCL	Geocomposite Clay Liner
GG	Geomembrane
GM	Geomembrane
LL	Liquid limit
NP	Needle punched
NWGT	Nonwoven
OMC	Optimum moisture content
PI	Plasticity index
PL	Plastic limit
PP	Polypropylene
PVC	Polyvinyl chloride
RIR	Reference Intensity Ratio
SC	Sandy clay
SI	Swell Index
WEV	Water entry value
WGT	Woven
WRC	Water retention curve

References

- Acikel, A.S., Gates, W.P., Singh, R.M., Bouazza, A., & Rowe, R.K. (2018). Insufficient initial hydration of GCLs from some subgrades: factors and causes. *Geotextiles and Geomembranes*, 46(6), 770-781. <http://dx.doi.org/10.1016/j.geotexmem.2018.06.007>.
- Anderson, R., Rayhani, M.T., & Rowe, R.K. (2012). Laboratory investigation of GCL hydration from clayey sand subsoil. *Geotextiles and Geomembranes*, 31, 31-38. <http://dx.doi.org/10.1016/j.geotexmem.2011.10.005>.
- ASTM D422-63. (2007). *Standard test method for particle-size analysis of soils*. ASTM International, West Conshohocken, PA.
- ASTM D698. (2012). *Standard test methods for laboratory compaction characteristics of soil using standard effort (12 400 ft-lbf/ft³ (600 kN-m/m³))*. ASTM International, West Conshohocken, PA.
- ASTM D584. (2014). *Standard test methods for specific gravity of soil solids by water pycnometer*. ASTM International, West Conshohocken, PA.
- ASTM D5298. (2016). *Standard test method for measurement of soil potential (suction) using filter paper*. ASTM International, West Conshohocken, PA.
- ASTM D2487-17e1. (2017a). *Standard practice for classification of soils for engineering purposes (unified soil classification system)*. ASTM International, West Conshohocken, PA.
- ASTM D6913. (2017b). *Standard test methods for particle-size distribution (gradation) of soils using sieve analysis*. ASTM International, West Conshohocken, PA.
- ASTM D4318. (2017c). *Standard test methods for liquid limit, plastic limit, and plasticity index of soils*. ASTM International, West Conshohocken, PA.
- ASTM D5261. (2018a). *Standard test method for measuring mass per unit area of geotextiles*. ASTM International, West Conshohocken, PA.
- ASTM D5993-18. (2018b). *Standard test method for measuring mass per unit area of geosynthetic clay liners*. ASTM International, West Conshohocken, PA.
- ASTM D7503. (2018c). *Standard test method for measuring the exchange complex and cation exchange capacity of inorganic fine-grained soils*. ASTM International, West Conshohocken, PA.
- ASTM D2216-19. (2019a). *Standard test methods for laboratory determination of water (moisture) content of soil and rock by mass*. ASTM International, West Conshohocken, PA.
- ASTM D5890. (2019b). *Standard test method for swell index of clay mineral component of geosynthetic clay liners*. ASTM International, West Conshohocken, PA.
- ASTM D5891. (2019c). *Standard test method for fluid loss of clay component of geosynthetic clay liners*. ASTM International, West Conshohocken, PA.
- ASTM D5887. (2020a). *Standard test method for measurement of index flux through saturated geosynthetic clay liner specimens using a flexible wall permeameter*. ASTM International, West Conshohocken, PA.
- ASTM D6496-03. (2020b). *Standard test method for determining average bonding peel strength between top and bottom layers of needle-punched geosynthetic clay liners*. ASTM International, West Conshohocken, PA.
- ASTM D1776. (2020c). *Standard practice for conditioning and testing textiles*. ASTM International, West Conshohocken, PA.
- ASTM D6768. (2020d). *Standard test method for tensile strength of geosynthetic clay liners*. ASTM International, West Conshohocken, PA.
- ASTM D6469. (2020e). *Standard guide for microbial contamination in fuels and fuel systems*. ASTM International, West Conshohocken, PA.
- Azad, F.M., Rowe, R.K., El-Zein, A., & Airey, D.W. (2011). Laboratory investigation of thermally induced desiccation of GCLs in double composite liner systems. *Geotextiles and Geomembranes*, 29(6), 534-543. <http://dx.doi.org/10.1016/j.geotexmem.2011.07.001>.
- Barroso, M., Touze-Foltz, N., von Maubeugec, K., & Pierson, P. (2006). Laboratory investigation of flow rate through composite liners consisting of a geomembrane, a GCL and a soil liner. *Geotextiles and Geomembranes*, 24(3), 139-155. <http://dx.doi.org/10.1016/j.geotexmem.2006.01.003>.
- Beddoe, R.A., Take, W.A., & Rowe, R.K. (2011). Water-retention behavior of geosynthetic clay liners. *Journal of Geotechnical and Geoenvironmental Engineering*, 137(11), 1028-1038. [http://dx.doi.org/10.1061/\(ASCE\)GT.1943-5606.0000526](http://dx.doi.org/10.1061/(ASCE)GT.1943-5606.0000526).

- Bouazza, A., Ali, M.A., Gates, W.P., & Rowe, R.K. (2017). New insight on geosynthetic clay liner hydration: the key role of subsoils mineralogy. *Geosynthetics International*, 24(2), 139-150. <http://dx.doi.org/10.1680/jgein.16.00022>.
- Bradshaw, S.L., & Benson, C.H. (2014). Effect of municipal solid waste leachate on hydraulic conductivity and exchange complex of geosynthetic clay liners. *Journal of Geotechnical and Geoenvironmental Engineering*, 140(4), 04013038. [http://dx.doi.org/10.1061/\(ASCE\)GT.1943-5606.0001050](http://dx.doi.org/10.1061/(ASCE)GT.1943-5606.0001050).
- Bradshaw, S.L., Benson, C.H., & Scalia IV, J. (2013). Hydration and cation exchange during subgrade hydration and effect on hydraulic conductivity of geosynthetic clay liners. *Journal of Geotechnical and Geoenvironmental Engineering*, 139(4), 526-538. [http://dx.doi.org/10.1061/\(ASCE\)GT.1943-5606.0000793](http://dx.doi.org/10.1061/(ASCE)GT.1943-5606.0000793).
- Chamindu Deepagoda, T.K.K., Moldrup, P., Jensen, M.P., Jones, S.B., de Jonge, L.W., Schjønning, P., Scow, K., Hopmans, J.W., Rolston, D.E., Kawamoto, K., & Komatsu, T. (2012). Diffusion aspects of designing porous growth media for earth and space. *Soil Science Society of America Journal*, 76, 1564-1578. <http://dx.doi.org/10.2136/sssaj2011.0438>.
- Chevrier, B., Cazaux, D., Didier, G., Gamet, M., & Guyonnet, D. (2012). Influence of subgrade, temperature and confining pressure on GCL hydration. *Geotextiles and Geomembranes*, 33, 1-6. <http://dx.doi.org/10.1016/j.geotexmem.2012.02.003>.
- Costa, A.M., Alfaia, R.G., & Campos, J.C. (2019). Landfill leachate treatment in Brazil: an overview. *Journal of Environmental Management*, 232, 110-116. <http://dx.doi.org/10.1016/j.jenvman.2018.11.006>.
- Dish, D.L. (2015). Quantitative X-ray diffraction analysis of soils. In J.E.A. Chair & J.W. Stucki (Eds.), *Quantitative methods in soil mineralogy* (pp. 267-295). Madison: Soil Science Society of America. <http://dx.doi.org/10.2136/1994.quantitativemethods.c9>.
- Durner, W. (1994). Hydraulic conductivity estimation for soils with heterogeneous pore structure. *Water Resources Research*, 30(2), 211-223. <http://dx.doi.org/10.1029/93WR02676>.
- Fredlund, D.G., & Xing, A. (1994). Equations for the soil-water characteristic curve. *Canadian Geotechnical Journal*, 31(4), 521-532. <http://dx.doi.org/10.1139/t94-061>.
- Geosynthetic Institute. (2016). *GRI-GCL3 standard specification test methods, required properties, and testing frequencies of Geosynthetic Clay Liners (GCLs)*. Folsom, PA: Geosynthetic Institute.
- Guyonnet, D., Touze-Foltz, N., Norotte, V., Pothier, C., Didier, G., Gailhanou, H., Blanc, P., & Warmont, F. (2009). Performance-based indicators for controlling geosynthetic clay liners in landfill applications. *Geotextiles and Geomembranes*, 27(5), 321-331. <http://dx.doi.org/10.1016/j.geotexmem.2009.02.002>.
- Hoai, T.T., & Mukunoki, T. (2020). Combined effects of ammonium permeation and dry-wet cycles on the hydraulic conductivity and internal properties of geosynthetic clay liners. *Geotextiles and Geomembranes*, 48(6), 912-927. <http://dx.doi.org/10.1016/j.geotexmem.2020.07.007>.
- Hosney, M.S., Brachman, R.W., & Rowe, K.R. (2016). Hydration of a GCL with powdered bentonite. In *Proceedings of the 6th European Geosynthetics Congress*, Ljubljana, Slovenia.
- Koerner, R.M., & Koerner, G.R. (2005). *In-situ separation of GCL panels beneath exposed geomembranes* (GRI White Paper, No. 5). Folsom, PA: Geosynthetic Institute.
- Liu, Y., Bouazza, A., Gates, W.P., & Rowe, R.K. (2015). Hydraulic performance of geosynthetic clay liners to sulfuric acid solutions. *Geotextiles and Geomembranes*, 43(1), 14-23. <http://dx.doi.org/10.1016/j.geotexmem.2014.11.004>.
- Maignien, R. (1966). *Review of research on laterites*. New York: Transportation Research Board.
- Marinho, F.A., & Gomes, J.E.S. (2012). The effect of contact on the filter paper method for measuring soil suction. *Geotechnical Testing Journal*, 35(1), 172-181. Retrieved in September 22, 2023, from <https://www.astm.org/gtj103571.html>
- Meer, S.R., & Benson, C.H. (2007). Hydraulic conductivity of geosynthetic clay liners exhumed from landfill final covers. *Journal of Geotechnical and Geoenvironmental Engineering*, 133(5), 550-563. [http://dx.doi.org/10.1061/\(ASCE\)1090-0241\(2007\)133:5\(550\)](http://dx.doi.org/10.1061/(ASCE)1090-0241(2007)133:5(550)).
- Portelinha, F.H.M., & Zornberg, J.G. (2017). Effect of infiltration on the performance of an unsaturated geotextile-reinforced soil wall. *Geotextiles and Geomembranes*, 45(3), 211-226. <http://dx.doi.org/10.1016/j.geotexmem.2017.02.002>.
- Portelinha, F.H.M., Correia, N.S., & Daciolo, L.V.P. (2020). Impact of temperature on immediate and secondary compression of MSW with high and low food contents. *Waste Management*, 118, 258-269. <http://dx.doi.org/10.1016/j.wasman.2020.08.044>.
- Rayhani, M.T., Rowe, R.K., Brachman, R.W.I., Take, W.A., & Siemens, G. (2011). Factors affecting GCL hydration under isothermal conditions. *Geotextiles and Geomembranes*, 29(6), 525-533. <http://dx.doi.org/10.1016/j.geotexmem.2011.06.001>.
- Rouf, M.A., Bouazza, A., Singh, R.M., Gates, W.P., & Rowe, R.K. (2016). Water vapour adsorption and desorption in GCLs. *Geosynthetics International*, 23(2), 86-99. <http://dx.doi.org/10.1680/jgein.15.00034>.
- Rowe, R.K. (2020). Geosynthetic clay liners: perceptions and misconceptions. *Geotextiles and Geomembranes*, 48(2), 137-156. <http://dx.doi.org/10.1016/j.geotexmem.2019.11.012>.
- Rowe, R.K., & Li, T.K. (2021). Influence of pore water chemistry on GCL self-healing with hydration from silica sand. *Geotextiles and Geomembranes*, 49(4), 871-894. <http://dx.doi.org/10.1016/j.geotexmem.2020.12.007>.
- Rowe, R.K., Rayhani, M.T., Take, W.A., Siemens, G., & Brachman, R.W.I. (2011). GCL hydration under simulated daily thermal cycles. *Geosynthetics International*, 18(4), 196-205. <http://dx.doi.org/10.1680/gein.2011.18.4.196>.
- Rowe, R.K., Rayhani, M.T., Take, W.A., Siemens, G., & Brachman, R.W.I. (2013). Physical modelling of nonwoven/nonwoven GCL shrinkage under simulated field conditions. *Geotextiles and Geomembranes*, 40, 12-19. <http://dx.doi.org/10.1016/j.geotexmem.2013.07.008>.

- Rowe, R.K., Garcia, J.D.D., Brachman, R.W.I., & Hosney, M.S. (2019). Chemical interaction and hydraulic performance of geosynthetic clay liners isothermally hydrated from silty sand subgrade. *Geotextiles and Geomembranes*, 47(6), 740-754. <http://dx.doi.org/10.1016/j.geotexmem.2019.103486>.
- Sarabian, T., & Rayhani, M.T. (2013). Hydration of geosynthetic clay liners from clay subsoil under simulated field conditions. *Waste Management*, 33(1), 67-73. <http://dx.doi.org/10.1016/j.wasman.2012.08.010>.
- Silva, J.W.B., Portelina, F.H.M., & Correia, N.S. (2022). Laboratory investigation of GCL hydration from Lateritic subsoils. *Geotextiles and Geomembranes*, 50, 946-960. <http://dx.doi.org/10.1016/j.geotexmem.2022.06.002>.
- Silva, N.F., Schoeler, G.P., Lourenço, V.A., Souza, P.L., Caballero, C.B., Salamoni, R.H., & Romani, R.F. (2020). First order models to estimate methane generation in landfill: a case study in south Brazil. *Journal of Environmental Chemical Engineering*, 8(4), 104053. <http://dx.doi.org/10.1016/j.jece.2020.104053>.
- Thiel, R., & Richardson, D.N. (2005). Concern for GCL shrinkage when installed on slopes. In *Geosynthetics Research and Development in Progress (GRI-18): Geo-Frontiers 2005*. Reston: American Society of Civil Engineers.
- Thiel, R., Giroud, J.P., Erickson, R., Criley, K., & Bryk, J. (2006). Laboratory measurements of GCL shrinkage under cyclic changes in temperature and hydration conditions. In *Proceedings of the 8th International Conference on Geosynthetics* (pp. 2-7). Rotterdam: Millpress.
- Yesiller, N., Hanson, J.L., Risken, J.L., Benson, C.H., Abichou, T., & Darius, J.B. (2019). Hydration fluid and field exposure effects on moisture-suction response of geosynthetic clay liners. *Journal of Geotechnical and Geoenvironmental Engineering*, 145(4), 04019010. [http://dx.doi.org/10.1061/\(ASCE\)GT.1943-5606.0002011](http://dx.doi.org/10.1061/(ASCE)GT.1943-5606.0002011).
- Yu, B., & El-Zein, A. (2020). Irrigated composite liner designs for fast hydration and prevention of thermal desiccation of geosynthetics clay liners. *Geotextiles and Geomembranes*, 48(6), 950-961. <http://dx.doi.org/10.1016/j.geotexmem.2020.08.004>.